Progress In Electromagnetics Research Letters, Vol. 50, 79–84, 2014

Compact Dual-Band Microstrip BPF with Multiple Transmission Zeros for Wideband and WLAN Applications

Hong-Li Wang, Hong-Wei Deng, Yong-Jiu Zhao, and Hao Liu

Abstract—In this letter, a novel compact dual-band microstrip bandpass filter (BPF) with multiple transmission zeros is proposed using the third-order interdigital structure and dual-mode short stub center-loaded resonator (DSLR) for wideband and WLAN applications. The high impedance feedline for the filter with the folded DSLR can function as the quarter-wavelength resonator (QWR) for the third-order interdigital filter. Meanwhile, the folded DSLR can be adopted without an evident increase of the size of the compact interdigital filter. Three transmission zeros between two passbands and in the lower- and upper-stopbands can be created due to the cross coupling between two high impedance feedlines as well as between the input and output, and the intrinsic characteristic of the DSLR. Further, two inverse QWR coupling short stubs with different size loaded in the $50\,\Omega$ feedlines can generate four transmission zeros to improve the isolation and deepen the stopband. Finally, a compact dual-band BPF prototype is designed, and good agreement can be obtained between measured and simulated results.

1. INTRODUCTION

Recently, various dual-band BPFs have been extensively studied and developed to meet requirements in modern multiband wireless communication systems, such as GSM, Wimax, and WLAN. Much research work was conducted, and various design approaches were proposed to design the dual-band filter. Among them, two kinds of methods are popular. The first method is to utilize a single resonator with controllable resonant frequencies, such as patches/loops resonators with perturbation structures, stepped-impedance resonators, and stub-loaded resonators [1]. The main disadvantage of the filters is that the bandwidths of dual bands can hardly be individually met. The second method is to combine two sets of different resonators with common input and output. The specification of the dual passbands can be individually met, but the structures are relatively complicated [2]. Moreover, most of the aforementioned filters [1, 2] are aimed at narrow band design (e.g., less than 10%). According to recent technical trends of wireless systems, wideband or UWB systems for high-speed and wireless communications with low power consumption are actively researched worldwide. Lately, some dual-band BPFs with single- or dual-wideband passbands were presented by adopting new design approaches or structures [5–12]. Although the BPFs reported in [3–6] exhibit their own merits, but they also suffer from many drawbacks, i.e., large circuit area [3], complex circuit topology [4], etched ground plane [5], poor passband selectivity and isolation [6]. In [7], a compact and wide upper-stopband single-wideband BPF with fractional bandwidth (FBW) of 16% for wideband passband was designed by using second-order combline structure and DSLR. However, the bandwidth for the wideband passband cannot be further widened easily, for only a part of the QWR is coupled to the I/O feedline. The BPFs in [8, 9] possess single plane configuration, compact size and high electrical performance simultaneously, however, it is difficult to individually meet the center frequencies and bandwidths of dual bands.

Received 10 November 2014, Accepted 2 December 2014, Scheduled 10 December 2014

* Corresponding author: Hong-Wei Deng (hwdeng@nuaa.edu.cn).

The authors are with the Key Laboratory of Radar Imaging and Microwave Photonics (Nanjing Univ. Aeronaut. Astronaut.), Ministry of Education, College of Electronic and Information Engineering, Nanjing University of Aeronautics and Astronautics, Nanjing 210016, China.

In this letter, a compact, high selectivity and isolation dual-band microstrip BPF for wideband and WLAN applications is proposed using the third-order interdigital structure and folded DSLR. The high impedance feedlines for the WLAN filter with the folded DSLR can function as the QWRs for the third-order interdigital wideband filter. Multiple transmission zeros can be created to sharpen the skirt, improve the isolation and deepen the stopband, due to two inverse QWR coupling short stubs with different size, the intrinsic characteristics of the DMR and the cross coupling between two high impedance feedlines as well as between the input and output. Finally, a compact dual-band BPF for wideband and WLAN passbands with 1 dB FBW of 75 and 5% is designed and fabricated. The measured results agree well with the simulated ones.

2. DUAL-BAND BPF WITH THIRD-ORDER INTERDIGITAL STRUCTURE AND FOLDED DSLR

The interdigital filter has been widely researched for its attractive features like compact structure, low loss and wide upper-stopband (the first spurious passband at around three times). According to the analysis in [10], the interdigital filter with the open terminating microstrip lines at the ends can achieve very wide bandwidth (greater than 30% FBW). In this case, all of the microstrip line elements serve as resonators, including the open terminating microstrip line, which are quarter-wavelength long at the center frequency. Figs. 1(a) and 1(c) give the schematic and coupling scheme of the third-order interdigital filter (length: l_1, width: w_1, gap: g_1) with the open terminating microstrip lines, respectively. The interdigital filter is simulated with HFSS and Fig. 2 illustrates the simulated insertion losses with varied g_1. The geometrical parameters of the microstrop line element centered at 3 GHz are: $l_1 = 17.8$ mm, $w_1 = 0.3$ mm. The substrate used herein is RT/Duriod 5880 with a thickness of 0.508 mm, permittivity of 2.2 and loss tangent of 0.0009. It is found that the bandwidth gets wider, as the gap g_1 become smaller. Thus, the passband center frequency can be determined by the l_1 and the desired bandwidth can be obtained by adjusting the g_1. Meanwhile, the filter has two transmission zeros T_{z1}, T_{z2} near the lower and upper passband edges, which result from the source-load coupling between the input and output and the cross coupling between two open terminating microstrip lines, respectively.

Figure 1(b) shows a folded DSLR composed of one short stub $(l_3, 2w_1)$ loaded at the centre plane and a high impedance microstrip line $(2l_2, w_1)$ parallel coupled to the open terminating microstrip lines. The open terminating microstrip line for the third-order interdigital filter as a QWR can function as

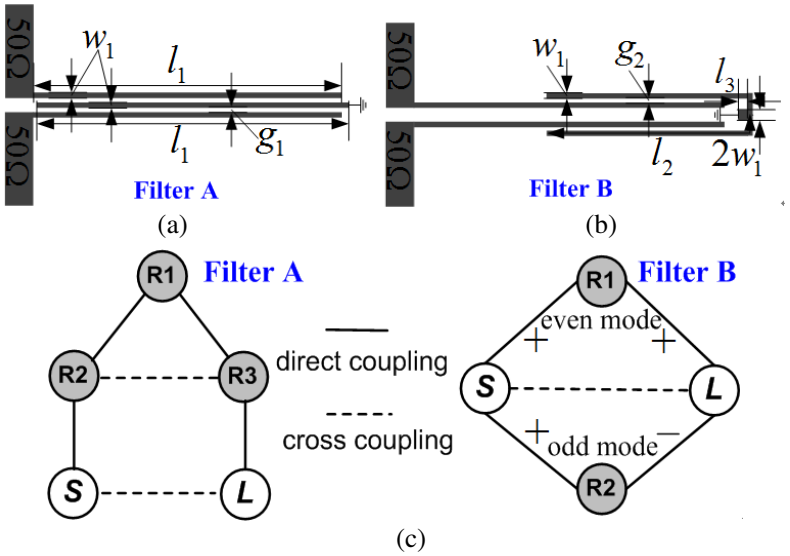

Figure 1. (a) and (b) schematics and (c) coupling schemes of the third-order interdigital filter (Filter A) and the filter with the folded DSLR (Filter B).

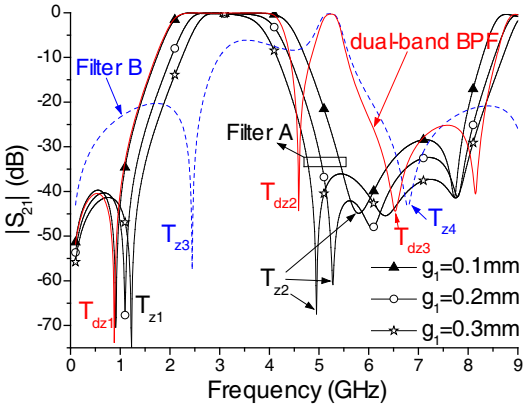

Figure 2. Simulated insertion losses of the Filter A with varied g_1, Filter B and dual-band filter.

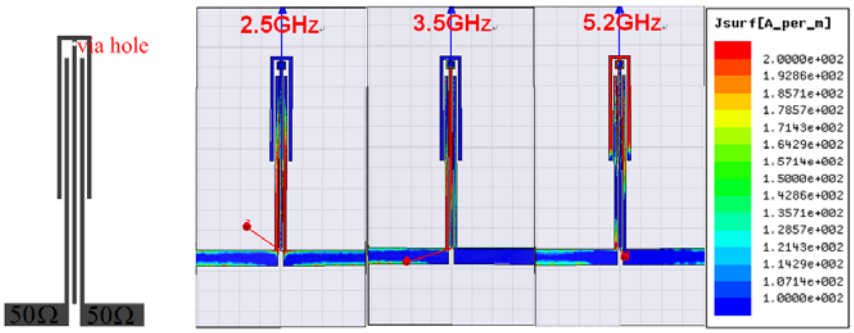

Figure 3. (a) Configuration and (b) current distributions of the dual-band filter with the third-order interdigital structure and folded DSLR.

high impedance microstrip feedline for the filter with the folded DSLR to supply the strong coupling. It is obvious that the folded DSLR has no evident increase of the circuit area. The resonator has two resonant frequencies (odd mode and even mode) in the desired passband, and the even-mode resonant frequency can be flexibly controlled by the short stub, whereas the odd-mode one is fixed [1, 2]. Thus, the $2l_1$ can be determined according to the given center frequency and bandwidth. And the desired bandwidth can be met by adjusting the l_3 Fig. 1(c) gives the coupling scheme of the filter with the folded DSLR. The source-load coupling is introduced by the open terminating microstrip lines and the input and output. The simulated insertion loss is illustrated in Fig. 2. The geometrical parameters of the filter centered at 5.2 GHz are fixed as: $l_2 = 11.3$ mm, $l_3 = 0.35$ mm, $g_1 = 0.2$ mm. Two transmission zeros T_{z3} and T_{z4} in the lower- and upper-stopbands are created due to the main path signal counteraction and the source-loaded coupling, respectively.

Further, a dual-band filter with third-order interdigital structure and folded DSLR is proposed and its configuration is shown in Fig. 3(a). The short stub of the folded DSLR is connected to the QWR. The simulated insertion loss and current distributions are given in Fig. 2 and Fig. 3(b), respectively. In Fig. 3(b), the current distributions at 2.5 and 3.5 GHz mainly concentrate at third-order interdigital structure, whereas the one at 5.5 GHz mainly concentrates at the folded DSLR and two open terminating microstrip lines. This implies that the dual-band filter still possesses the advantage of which the specification of the dual passbands can be individually met. However, it is found from Fig. 2 that the upper edge of the wideband passband gets lower, for the T_{zd2} created due to the main path signal counteraction is close to the wideband passband edge. Hence, the center frequency and bandwidth of the wideband passband need to be amended by simply varying the l_1 and g_1, respectively. Two other transmission zeros T_{dz1} and T_{dz3} is generated due to the source-loaded coupling and cross coupling

between two open terminating microstrip lines. By comparing with the Filter A and Filter B, the transmission zeros T_{dz2} and T_{dz3} move upwards due to the mutual loading effect of the folded DSLR and third-order interdigital structure.

3. DUAL-BAND BPF WITH QWR COUPLING SHORT STUBS

As well known, the short stub loaded in the 50 Ω feedlines which is about half-wavelength long, can be applied to generate new transmission zeros. As analyzed in [11], the inverse QWR tight coupled to the short stub, which can also generate new transmission zeros, has less effect on the first transmission zero generated by the short stub. To further improve the isolation and deepen the stopband, two inverse QWR coupling short stubs with different size in Fig. 4(a) are loaded in the 50 Ω feedlines. Fig. 5 gives the simulated insertion losses of the dual-band filter with two short stubs and two inverse QWR coupling short stubs. The two transmission zeros T_{dz4} and T_{dz5} in the lower- and upper-stopbands can be created by the short stubs denoted by l_4 and l_5, respectively, which can deepen the stopband. The inverse QWR1 (d_1, w_1) and QWR2 (d_2, w_1) can create two transmission zeros T_{dz6} near the upper edge of wideband passband and T_{dz7} near the lower edge of second passband, which can sharpen the skirt and improve the isolation. As shown in Fig. 6(a), a dual-band BPF is designed with 1 dB FBWs of 75% at 3.0 GHz for wideband passband and 5% at 5.2 GHz for WLAN passband.

The dual-band filter is fabricated and its photograph is shown in Fig. 4(b). The performance is measured by Agilent network analyzer N5230C. The simulated and measured frequency responses are illustrated in Fig. 6, and found in good agreement with each other. Measured central frequencies of

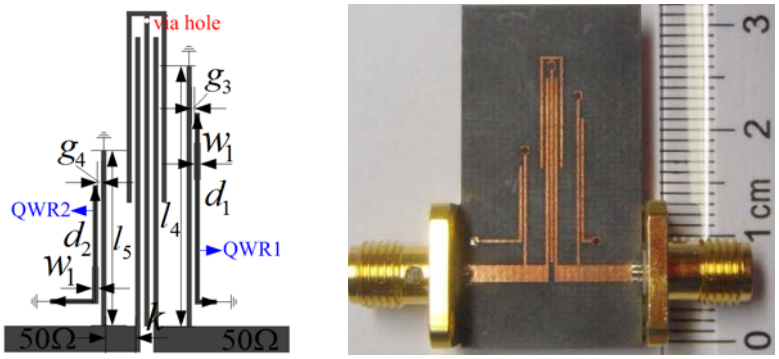

(a) (b)

Figure 4. (a) Configuration and (b) photograph of the dual-band BPF with the QWR coupling short stubs.

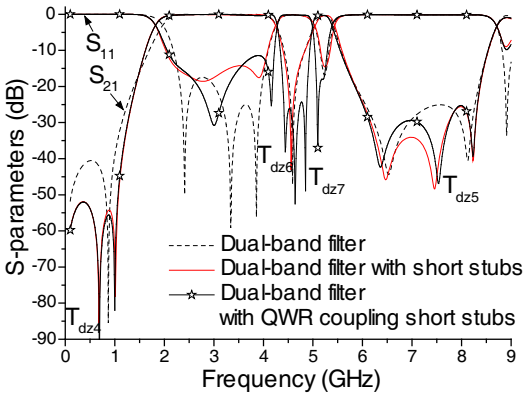

Figure 5. Simulated S-parameters of the dual-band BPF with the short stubs and QWR coupling short stubs.

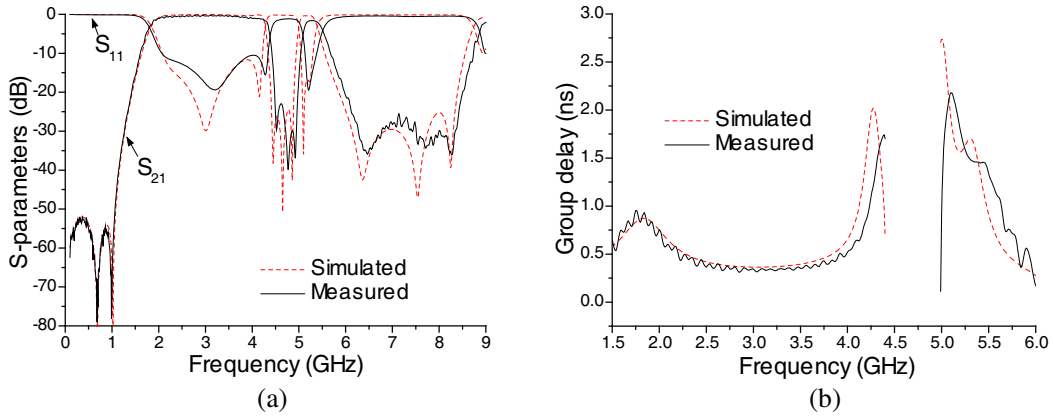

Figure 6. Simulated and measured frequency responses of the dual-band BPF with the QWR coupling short stubs. (a) S-parameters. (b) Group delay.

the wideband and WLAN passbands are about 3.1 and 5.2 GHz with 3 dB FBWs of 73.2% and 4.8% with return loss better than 10 dB. Three transmission zeros between two passbands are located at 4.52, 4.77 and 4.92 GHz resulting in high isolation, with an attenuation level of better than 30 dB. The lower- and upper-stopband rejection levels in experiment are better than 50 dB and 25 dB in the range of 0.1–1.06 GHz and 6.13–8.42 GHz, respectively. In Fig. 6(b), the measured group delay for wideband passband varies from 0.4 to 0.75 ns, which is quite small and flat, since only three resonators are used to form the passband. The measured group delay for WLAN passband varies from 1.35 to 1.75 ns. The group delay near the lower WLAN passband edge is very large, due to the strong cross coupling between two open terminating microstrip lines.

4. CONCLUSION

In this letter, a novel dual-band microstrip BPF with compact size, high selectivity and isolation is proposed using the third-order interdigital structure and folded DSLR for wideband and WLAN applications. The high impedance feedlines for the WLAN filter with the folded DSLR can function as the QWRs for the third-order interdigital wideband filter. Multiple transmission zeros can be generated to sharpen the skirt, improve the isolation and deepen the stopband. Good agreement between measured and simulated results demonstrates the validity of our proposed structure.

ACKNOWLEDGMENT

This work was supported by the Priority Academic Program Development of Jiangsu Higher Education Institutions (PAPD).

REFERENCES

1. Deng, H. W., Y. J. Zhao, X. S. Zhang, W. Chen, and J. K. Wang, "Compact and high selectivity dual-band dual-mode microstrip BPF with single stepped-impedance resonator," *Electron. Lett.*, Vol. 47, No. 5, 326–327, Mar. 2011.
2. Deng, H. W., Y. J. Zhao, L. Zhang, X. S. Zhang, and W. Zhao, "Dual-band BPF with DSIR and TSIR," *Electron. Lett.*, Vol. 46, No. 17, 1205–1206, Aug. 2010.
3. Liu, A.-S., T.-Y. Huang, and R.-B. Wu, "A dual wideband filter design using frequency mapping and stepped-impedance resonators," *IEEE Trans. Microw. Theory Tech.*, Vol. 56, No. 12, 2921–2929, Dec. 2008.

4. Qshima, S., K. Wada, R. Murata, and Y. Shimakata, "Multilayer dual-band bandpass filter in low-temperature co-fired ceramic substrate for ultra-wideband applications," *IEEE Trans. Microw. Theory Tech.*, Vol. 58, No. 3, 614–623, Mar. 2010.
5. Xin, J., W. Wu, and C. Miao, "Compact and sharp skirts microstrip dual-mode dual-band bandpass filter using a single quadruple-mode resonator (QMR)," *IEEE Trans. Microw. Theory Tech.*, Vol. 61, No. 3, 1104–1113, Mar. 2013.
6. Zhang, R. Q. and L. Zhu, "Synthesis and design of wideband dual-band bandpass filters with controllable in-band ripple factor and dual-band isolation," *IEEE Trans. Microw. Theory Tech.*, Vol. 61, No. 5, 1820–1828, May 2013.
7. Deng, H. W., Y. J. Zhao, Y. Fu, X. J. Zhou, and Y. Y. Liu, "Compact and high selectivity dual-band microstrip BPF with QWR and SLR," *Microwave and Optical Tech. Lett.*, Vol. 54, No. 12, 2702–2705, Dec. 2012.
8. Hsu, K.-W., C.-H. Chien, and W.-H. Tu, "Compact dual-wideband bandpass filter using asymmetrical resonator," *Electron. Lett.*, Vol. 49, No. 2, 123–124, Jan. 2013.
9. Xu, J., Y.-X. Ji, C. Miao, and W. Wu, "Compact single-/dual-wideband BPF using stubs loaded SIR (SsLSIR)," *IEEE Microw. Wireless Compon. Lett.*, Vol. 23, No. 7, 338–340, Jul. 2013.
10. Matthaei, G. L., "Interdigital band-pass filters," *IEEE Trans. Microw. Theory Tech.*, Vol. 10, No. 6, 479–461, Feb. 1962.
11. Deng, H. W., Y. J. Zhao, Y. Fu, J. Ding, and X. J. Zhao, "Compact and high isolation microstrip diplexer for broadband and WLAN application," *Progress in Electromagnetics Research*, Vol. 133, 133–555, 2013.